Proc. Natl. Acad. Sci. USA
Vol. 90, pp. 4996–5000, June 1993
Biochemistry

Feedback inhibition of fully unadenylylated glutamine synthetase from *Salmonella typhimurium* by glycine, alanine, and serine

(x-ray crystallography/protein structure/effector binding)

SHWU-HUEY LIAW, CLARK PAN, AND DAVID EISENBERG*

Molecular Biology Institute and Department of Chemistry and Biochemistry, University of California, Los Angeles, CA 90024

Contributed by David Eisenberg, December 28, 1992

ABSTRACT **Bacterial glutamine synthetase (GS; EC 6.3.1.2) was previously shown to be inhibited by nine end products of glutamine metabolism. Here we present four crystal structures of GS, complexed with the substrate Glu and with each of three feedback inhibitors. The GS of the present study is from *Salmonella typhimurium*, with Mn^{2+} ions bound, and is fully unadenylylated. From Fourier difference maps, we find that L-serine, L-alanine, and glycine bind at the site of the substrate L-glutamate. In our model, these four amino acids bind with the atoms they share in common (the "main chain" $^{+}NH_3$-CH-COO^{-}) in the same positions. Thus on the basis of our x-ray work, glycine, alanine, and serine appear to inhibit GS-Mn by competing with the substrate glutamate for the active site.**

Glutamine synthetase (GS) catalyzes the formation of glutamine from glutamate and ammonia with the concomitant hydrolysis of ATP into ADP and P_i. The amide group of glutamine serves as a nitrogen source for the biosynthesis of nitrogen-containing metabolites (1, 2). The original kinetic studies by Woolfolk and Stadtman showed that *Escherichia coli* GS was inhibited by nine end products of glutamine metabolism: serine, alanine, glycine, AMP, CTP, tryptophan, histidine, carbamoyl phosphate, and glucosamine 6-phosphate (3–5). Each inhibitor was found to inhibit part of the GS activity, and collectively they were found almost to abolish GS activity. These findings led Woolfolk and Stadtman to propose "cumulative feedback inhibition." In their model each inhibitor binds to a separate site, distinct from the catalytic site, and each is independent in its action.

The question of the number of distinct effector binding sites on the surface of GS was studied intensively in the 1970s. In addition to kinetic measurements, methods including NMR, EPR, fluorimetry, equilibrium binding, and calorimetry were all applied to study this complicated feedback regulatory system. Studies of equilibrium binding and of calorimetric measurement of AMP, L-tryptophan, L-alanine, and L-glutamate suggested that these effectors bind at separate sites on GS (6–8). Fluorescence measurements and NMR led to the conclusions that low- to unadenylylated GS possesses allosteric sites for amino acid inhibitors and that GS has different sites for L-glutamate, L-alanine, D-alanine, and glycine (9).

Different conclusions were reached by Dahlquist and Purich (10), who examined the interaction of low- to unadenylylated GS with the eight feedback inhibitors by magnetic resonance techniques. Their results suggested that the feedback inhibitors alanine, tryptophan, histidine, and glycine bound to the glutamate substrate site. Also, according to Rhee *et al.* (11), titration and kinetic data suggested that glycine can bind to both the L-alanine and D-alanine sites. A common site for L-glutamate and L-alanine appeared when the binding of L-glutamate to GS was measured in the presence of ADP and P_i (6, 9). Citing these studies and unpublished data, Stadtman and Ginsburg (2) concluded "there are separate sites on the enzyme for alanine, tryptophan, histidine, AMP, and CTP, whereas mutually exclusive binding occurs between glycine, serine, and alanine" (P. Z. Smyrniotis and E. R. Stadtman, unpublished data cited in review reference 2). And Rhee *et al.* (11) reviewed further evidence for separate sites of inhibition. In short, feedback inhibition of GS is a complicated regulatory system, worthy of continued study.

X-ray crystallography is well suited for the definition of binding sites. By x-ray methods, an initial atomic model for the 5616 residues of dodecameric unadenylylated GS from *Salmonella typhimurium* was determined at 3.5-Å resolution by Almassy *et al.* (12) and refined by Yamashita *et al.* (13). Recently a 2.8-Å-resolution atomic model has been refined based on x-ray diffraction data collected from one GS crystal of fine quality. This native model† is used here with the Fourier difference method to define the interactions of L-alanine, L-serine, L-glutamate, and glycine with fully unadenylylated GS-Mn from *S. typhimurium*.

MATERIALS AND METHODS

Purification of GS. GS for crystallization was isolated by ammonium sulfate precipitation and Cibracon Blue affinity column (14), whereas the protein for kinetic measurements was purified by ammonium sulfate precipitation (5). In the former method, ATP was used to elute GS from the column and could not be removed completely by extensive dialysis due to its high affinity for the enzyme. The bound ATP on GS could conceivably affect the kinetic measurements and hence was avoided.

Crystal Soaking and Data Collection. Fully unadenylylated crystals of GS from *S. typhimurium* were grown by the hanging-drop method of vapor diffusion (15). An effector was dissolved in the synthetic mother liquor containing 15 mM imidazole/HCl (pH 7.0), 3 mM $MnCl_2$, 3 mM spermine tetrahydrochloride, and 10% 2-methyl-2,4-pentanediol (MPD). Since the sudden replacement of mother liquor with synthetic mother liquor degrades the diffraction quality of GS crystals, half the volume of real mother liquor (5–10 μl) was replaced by the synthetic mother liquor containing one effector. In this way, L-serine, L-alanine, and glycine were added to GS crystals and allowed to diffuse for at least 1 day. Estimated final concentrations of L-glutamate, L-serine, L-alanine, and glycine were 10 mM, 30 mM, 15 mM, and 15 mM, respectively. X-ray data of GS–inhibitor complex crystals (Table 1) were collected with an R-AXIS-II image plate

The publication costs of this article were defrayed in part by page charge payment. This article must therefore be hereby marked "*advertisement*" in accordance with 18 U.S.C. §1734 solely to indicate this fact.

Abbreviation: GS, glutamine synthetase.
*To whom reprint requests should be addressed.
†The atomic coordinates and structure factors have been deposited in the Protein Data Bank, Chemistry Department, Brookhaven National Laboratory, Upton, NY 11973 (reference 1LGS).

Table 1. Summary of data collection of GS–effector complexes

Crystal	Resolution, Å	Unique/total reflections	R_{sym},* %	$\langle \Delta F \rangle / \langle F \rangle$,† %
GS	2.8	106,965/234,915	7.8	—
GS–Glu	2.8	110,184/170,218	6.0	17.8
GS–Ser	2.9	98,318/145,232	6.4	9.6
GS–Ala	2.8	93,308/147,344	7.9	12.0
GS–Gly	2.8	104,689/161,708	7.4	9.6
GS–Glu–Ala	2.9	90,491/136,568	6.4	16.6

*On intensity.
†Mean fractional isomorphous difference, $\Sigma || F_{PH}| - |F_P|| / \Sigma |F_P|$.

detector (Rigaku, Denko, Japan). All complex crystals were isomorphous with respect to the native GS crystals, having space group $C2$ and unit-cell dimensions a = 235.5 Å, b = 134.5 Å, c = 200.1 Å, and β = 102.8°.

Fourier Difference Maps, $F_{o(GS\text{–}effector)} - F_{o(GS)}$. Fourier difference maps with a 12-fold average, using Fourier coefficients $[F_{o(GS\text{–}effector)} - F_{o(GS)}]$, were calculated by using CCP4 programs (Science and Engineering Research Council Collaborative Computing Project no. 4, Daresbury Laboratory, Warrington, U.K.) implemented on a DEC VAX 4000 computer at the University of California, Los Angeles. Phases of the 2.8-Å native GS model were used as the initial phases of the complexes, as justified by the crystal isomorphism. The 12-fold averaged difference maps displayed little noise above the 1σ contour level.

GS Assay. The enzymatic activity of GS can be measured by the formation of P_i in the biosynthetic reaction (16) and by the formation of γ-glutamylhydroxamate in the glutamyl transfer reaction (17). In order to compare with the kinetic data of Woolfolk and Stadtman (5), kinetic measurements were performed under conditions which were virtually identical to their conditions.

For the biosynthetic assay, 80 μl of reaction mixture containing 100 mM imidazole/HCl (pH 7.0), 100 mM $MgCl_2$, 100 mM NH_4Cl, 20 mM ATP, and various concentrations of L-glutamate was mixed with 80 μl of GS at 37°C to initiate the reaction. After 9 min, the reaction was terminated by adding 640 μl of 1% $FeSO_4$ in 7.5 mM H_2SO_4; 10 sec later, a faint blue color was developed by the addition of 60 μl of 6.6% ammonium molybdate/3.75 M H_2SO_4. The P_i produced was measured from OD_{660} 1 min after ammonium molybdate was added.

For the transferase assay, 250 μl of reaction mixture containing 150 mM triethanolamine, 50 mM dimethyl glutarate, 300 mM KCl, 20 mM $KAsO_4$, 20 mM NH_2OH·HCl, 0.4 mM ADP, 0.4 mM $MnCl_2$, and various concentrations of L-glutamate were combined with 100 μl of GS at 37°C to start the reaction. After 10 min, the reaction was stopped by adding 1 ml of 3.3% $FeCl_3$/2% trichloroacetic acid/0.25 M HCl. The OD_{540} was read 3 min later to determine the amount of glutamylhydroxamate produced.

RESULTS

Model Building of Effectors into Fourier Difference Maps. Five 12-fold averaged Fourier difference maps are shown in Fig. 1. All the strongest peaks in these clear difference maps at the 2σ contour level appear at the same position in the active site. Atomic models of L-glutamate, glycine, L-alanine, and L-serine were built into the strongest density peaks in their respective difference maps (Fig. 1 *a–d*). The atomic model of glycine was built first because the density peak suggests the orientation of glycine. The main chain of L-glutamate was built at the same position as glycine because of the common atoms they have. The side chain of L-glutamate was built into difference density projecting toward the ATP binding site for the formation of γ-glutamyl phosphate in the biosynthetic reaction (2, 3). The atomic models of L-alanine and L-serine were built in their difference maps, based on the glycine model. The overlapping atomic models (Fig. 1*f*) constitute evidence that these feedback inhibitors bind to the main-chain region of the L-glutamate binding site.

In the difference map of GS–Ser, in addition to the strongest peak assigned L-serine as explained in the preceding paragraph, there is a positive density peak and a negative peak on opposite sides of Asn-264 (Fig. 1*g*). The positive peak cannot be the L-serine, because its size is too small to fit the atomic model of the effector and because it overlaps partially the side chain of Asn-264. The two peaks can, however, be interpreted as the motion of Asn-264 away from the serine site and toward the ε-amino group of Lys-176. This movement can relieve overlap of the amide group of Asn-264 with the α-amino group of serine (1.9 Å).

The positive peaks and the negative peaks in the difference map $[F_{o(GS\text{–}Ser)} - F_{o(GS)}]$ (Fig. 1*g*) along residues 322–329 show that this segment becomes more ordered upon serine binding. There is little electron density in the averaged $(2F_o - F_c)$ map of native GS but there is density in that of GS–Ser (Fig. 1*h*). The formation of one hydrogen bond between the γ-carboxylate group of Glu-327 and the β-hydroxyl group of serine might stabilize this segment. However, this segment does not seem to be similarly stabilized in the GS–Glu complex, perhaps because of the electrostatic repulsion between the substrate glutamate and the Glu-327 residue.

The density peak of L-serine in its difference map can be interpreted in terms of the model of Fig. 2. As judged by atom types and separation, the α-carboxylate group of L-serine forms hydrogen bonds with the guanidino group of Arg-321. Similarly, the α-amino group of L-serine forms a hydrogen bond with the carbonyl group of Gly-265 and a hydrogen bond with the γ-carboxylate group of Glu-131. The β-hydroxyl group of L-serine may form one hydrogen bond with the γ-carboxylate group of Glu-327. The interactions of L-alanine and glycine with GS are very similar to those of serine except that they lack the interactions of the β-hydroxyl group.

Kinetic Measurements of GS. To reconcile our structural studies with the earlier models for feedback control of GS, we investigated the inhibition of GS by glycine, L-alanine, and L-serine by both the biosynthetic assay and the glutamyltransferase assay (5). Our kinetic studies were carried out with the protocol of Woolfolk and Stadtman (5) with little modification. The only difference is that we used a smaller volume—0.16 ml of assay mixture and 0.64 ml of stop mixture instead of 0.2 ml and 1.8 ml, respectively—so that the blue color would be less diluted.

Studies by the biosynthetic assay (data not shown) present a complicated picture, but the transferase assay (Fig. 3) gives a simple result of competitive inhibition kinetics for glycine, L-alanine, and L-serine. With the biosynthetic assay, both K_m and V_{max} experience changes at low inhibitor concentrations ("uncompetitive"), and V_{max} is changed at higher inhibitor concentrations ("noncompetitive"). But with the transferase assay, only the apparent K_m changes in the presence of alanine, glycine, and serine (competitive inhibition). The estimated K_i values for alanine, glycine, and serine are 0.16, 0.8, and 1.1 mM, respectively. Also, when the data are plotted in single reciprocal form ([glutamine]/velocity vs. [glutamine] at various serine, alanine, and glycine concentrations) parallel lines are observed with slopes of 25.2 ± 0.6, suggesting competitive inhibition.

DISCUSSION

Interactions of Glycine, L-Alanine, and L-Serine with GS. Comparison of the structures of GS–Ser, GS–Ala, and GS–Gly complexes with that of the GS–Glu complex (Fig. 1*e*) presents direct evidence for the similarity in binding to GS of these inhibitors and of glutamate. Based on the difference maps, L-serine, L-alanine, and glycine appear to occupy essentially

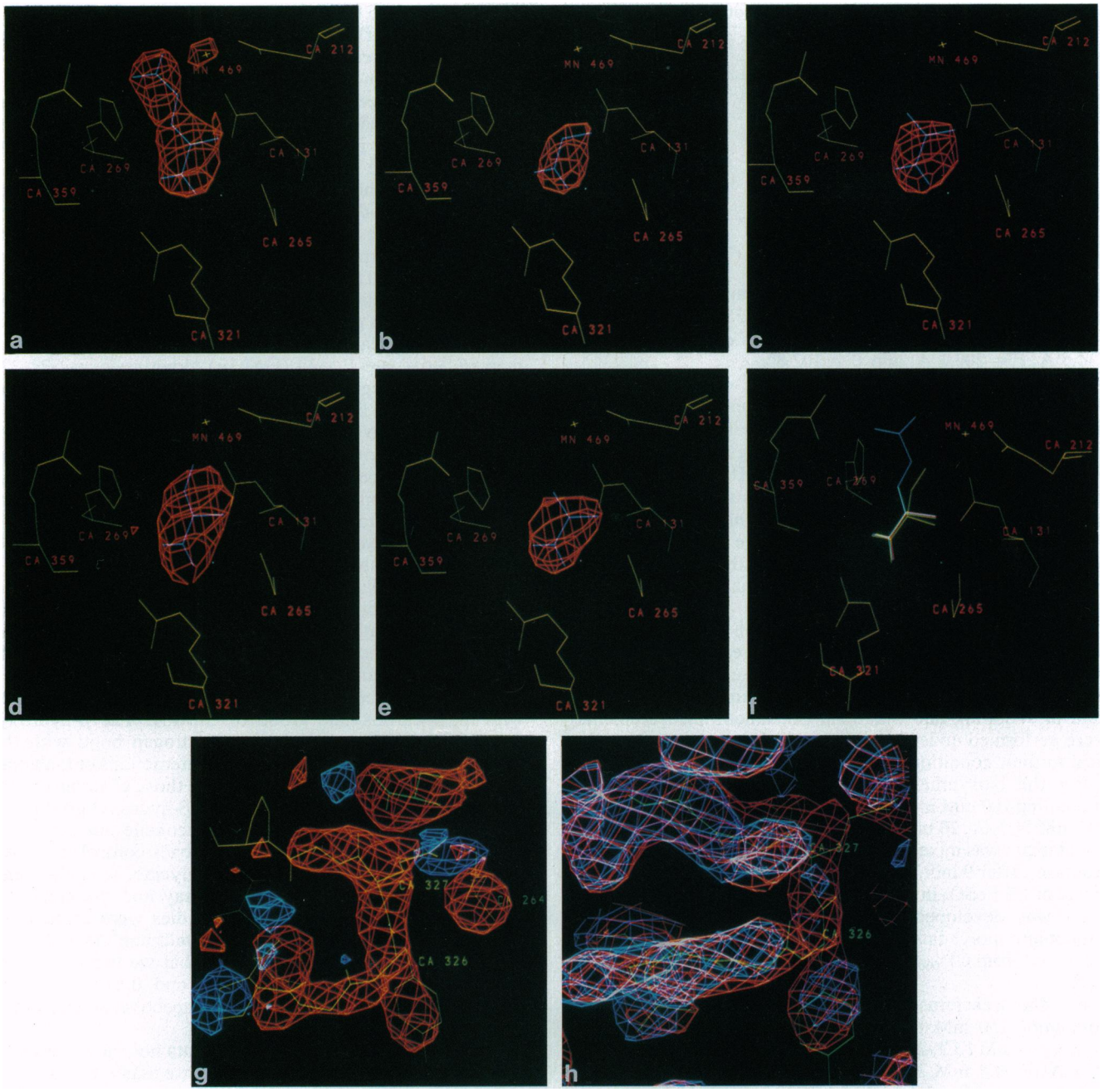

FIG. 1. The strongest peaks in the 12-fold averaged Fourier difference maps [$F_{o(GS\text{–effector})} - F_{o(GS)}$] before refinement. (*a*) $F_{o(GS\text{–Glu})} - F_{o(GS)}$. (*b*) $F_{o(GS\text{–Gly})} - F_{o(GS)}$. (*c*) $F_{o(GS\text{–Ala})} - F_{o(GS)}$. (*d*) $F_{o(GS\text{–Ser})} - F_{o(GS)}$. (*e*) $F_{o[GS\text{–(Glu+Ala)}]} - F_{o(GS)}$. (*f*) The atomic models: L-glutamate is shown in blue, L-serine in yellow, L-alanine in green, and glycine in red. These overlapping models suggest that L-glutamate, L-serine, L-alanine, and glycine occupy the same site for the atoms they have in common. (*g*) The difference map $F_{o(GS\text{–Ser})} - F_{o(GS)}$ in greater detail, but from a different point of view than *d*. The positive density map is shown in orange, the negative map in blue, and the GS atomic model in yellow. There are three positive density peaks at 1.2σ contour level; one is the serine peak with its atomic model; another, beside Asn-264, shows the movement of Asn-264 away from the serine site; the third implies that the segment 322–329 becomes more ordered. (*h*) $2F_o - F_c$ map of native GS is displayed in blue and that of the GS–Ser complex in red. In the native GS $2F_o - F_c$ map, virtually no density is observed in residues 326–327. However, the electron density for Tyr-327 and Glu-327 is seen in the map of the GS–Ser complex, indicating that these residues become more ordered upon serine binding.

the same site and might be expected to inhibit GS by competing for the active site against the substrate L-glutamate. This conclusion is consistent with the original notion of Woolfolk and Stadtman (5) about multiple feedback inhibition but suggests a mechanism for these inhibitors on GS–Mn which differ from theirs and from that of Rhee *et al.* (9). Our mechanism is consistent with the mechanism of Dahlquist and Purich (10) for alanine, glycine, and serine and with the mechanism based on the unpublished data of Smyrniotis and Stadtman cited in ref. 2. We note also that other authors were not studying fully unadenylylated GS–Mn from *S. typhimurium*, but rather *E. coli* GS in various states of adenylylation and with Mg^{2+} as well as Mn^{2+}. In a biochemical system as complicated as GS, these differences could conceivably account for some differences in effector action.

Kinetic Measurements of GS in the Presence of Glycine, L-Alanine, and L-Serine. The kinetic data from the transferase assay are consistent with inhibition of GS by L-alanine,

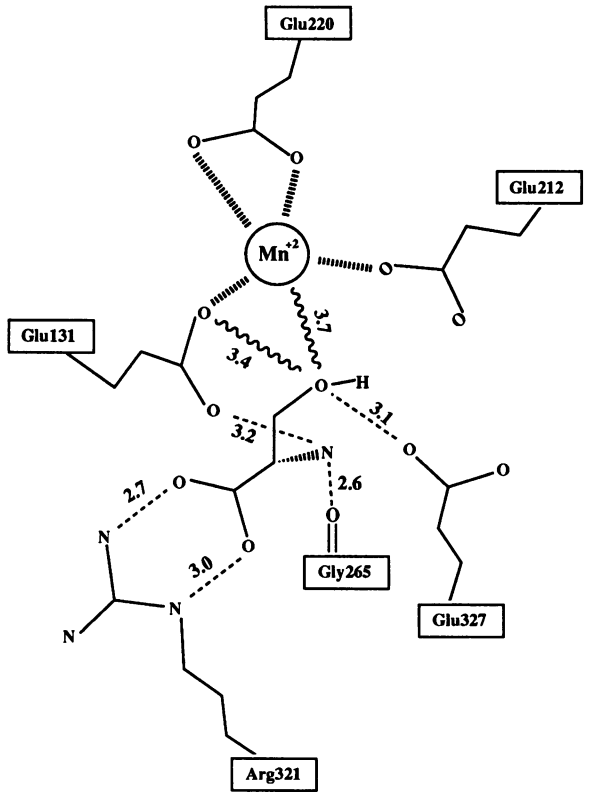

FIG. 2. Model for interactions of L-serine with GS as discussed in the text. Hydrogen bond lengths and other separations are shown by numbers (in angstroms). Glu-131, Glu-212, and Glu-220 are ligands for Mn^{2+}. It is uncertain that both oxygen atoms of Glu-220 coordinate to Mn^{2+}.

glycine, and L-serine by competition for the active site. The more complicated pattern of kinetics observed with the biosynthetic assay may be explained in two ways. The first explanation is metal dependence. The transferase assay uses GS–Mn whereas the biosynthetic assay uses GS–Mg, because completely unadenylylated GS from *S. typhimurium* and *E. coli* (18) has no biosynthetic activity in the presence of Mn^{2+}. Our crystal data were collected from GS–Mn, which presumably is the same GS–Mn form that carried out the transferase activity. However, Mg^{2+} and Mn^{2+} have markedly different effects on catalytic parameters and on the inhibitory response to different inhibitors (2, 18); thus they may stabilize different conformations of GS, and thus the biosynthetic assay may suggest a more complicated mode of catalysis for GS–Mg. Whether Mg^{2+} actually stabilizes a different conformation we will learn only when we determine the structure of GS–Mg.

The second explanation for the complicated behavior of the biosynthetic assay is the relative stabilities of complexes GS–ATP–Glu, GS–ADP–(P_i)–Glu, GS–ATP–inhibitor, and GS–ADP–(P_i)–inhibitor. The K_m or K_i values (19) and the dissociation constants (8, 9, 20–22) indicate that the binding affinities of ATP and ADP for GS are stronger than those of glutamate and other amino acids. Also, ATP is believed to be the first substrate to bind to GS (19). Thus glutamate, serine, alanine, and glycine are competing to bind to GS–ATP instead of GS. The kinetics of the biosynthetic reaction may indicate that glycine, alanine, and serine form more stable complexes with GS–ADP, and less stable with GS–ATP. If so, then in the transferase assay, competition is observed because both the substrate and the inhibitor bind to the same enzyme form, namely GS–ADP–P_i, or GS–ADP–AsO_4^-. However, if glycine, alanine, and serine do not bind as strongly to GS–ATP, a noncompetitive component to the

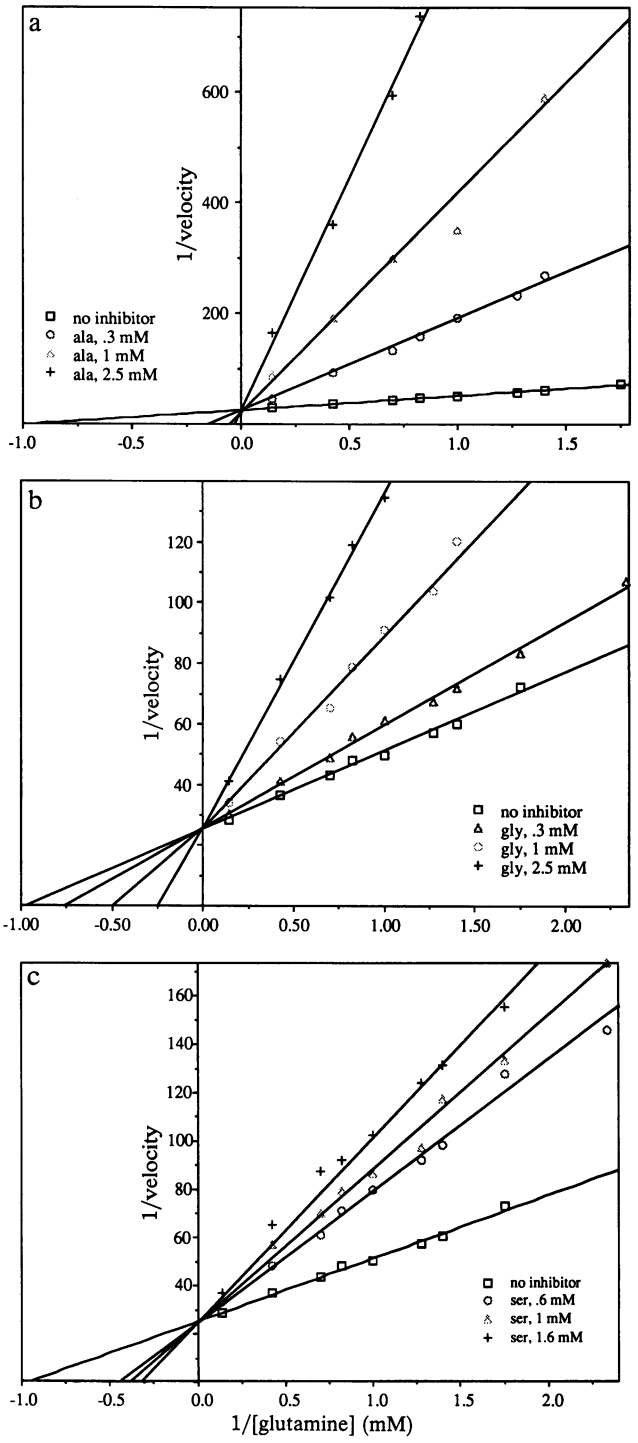

FIG. 3. Kinetic studies of L-alanine, L-serine, and glycine using the transferase assay for GS–Mn. Double-reciprocal plots are shown in which 1/velocity is plotted as a function of 1/[glutamine] in the presence of L-alanine (*a*), glycine (*b*), or L-serine (*c*). These kinetic data suggest that L-serine, L-alanine, and glycine are competitive inhibitors of GS–Mn with respect to L-glutamine.

inhibition will be observed. This pattern of a noncompetitive component to the kinetics of an enzyme that is inhibited at the active site was observed for the inhibition of alcohol dehydrogenase by auramine O (23). In that case, noncompetitive inhibition in the initial rate studies was explained by the ability of auramine O to form a ternary complex with enzyme–NAD^+ and enzyme–NADH binary complexes.

A noncompetitive component in the biosynthetic assay is supported by the dissociation constants (8, 9, 20–22). These

dissociation constants suggest that GS–Mg–ATP–Glu is more stable than GS–Mg–ADP–P_i–Glu, whereas GS–Mg–ATP–Ala is less stable than GS–Mg–ADP–P_i–Ala. Previous measurements also show that in the presence of GS–Mg–ADP, alanine enhances P_i binding 20-fold, whereas glutamate decreases P_i binding by a factor of 25 (8). These relative stabilities suggest that the noncompetitive component of the GS biosynthetic reaction in the presence of L-alanine may be consistent with inhibition of L-alanine at the GS active site, in analogy with the case of alcohol dehydrogenase (23). Further, the surprising observation of noncompetitive inhibition by the product L-glutamine in the biosynthetic reaction (19) could have a similar explanation.

The Fourier Difference Map $F_{o[GS-(Glu+Ala)]} - F_{o(GS)}$. The structures of the complexes GS–Gly, GS–Ser, and GS–Ala were determined in the absence of any substrate. Could these inhibitors bind to a second site in the presence of glutamate? The crystal structure of GS–Mn soaked with both 10 mM L-glutamate and 15 mM L-alanine has been determined in order to investigate the existence of a second binding site or to confirm the competitive inhibition mode between glutamate and alanine. According to our kinetic data, about 60% of the biosynthetic activity of GS–Mg in the presence of 10 mM L-glutamate is lost due to the inhibition by 15 mM L-alanine. As presented in Fig. 1 *a* and *c*, a peak is observed in the difference map of GS–Glu (10 mM L-glutamate), and a peak in the same site is also found in that of GS–Ala in the presence of 15 mM L-alanine.

In the difference map $\{F_{o[GS-(Glu+Ala)]} - F_{o(GS)}\}$, the strongest peak appears at the main-chain region of the L-glutamate binding site (Fig. 1*e*). No other density peak for a second binding site is observed. The size of the strongest peak is well fit by the atomic model of L-alanine. Also, density for the side chain of L-glutamate is not observed. This map suggests that most of the glutamate sites are occupied by alanine, not by glutamate. Thus this result is consistent with our hypothesis that L-alanine is a competitive inhibitor with respect to glutamate and its affinity for GS is not substantially lower than that of glutamate.

Is There a Conformational Change upon Inhibitor Binding? Further evidence supporting classical competitive inhibition for GS is provided by an analysis of quaternary and tertiary changes. There is no significant conformational change induced by the binding of these three inhibitors other than the movement of Asn-264. The large-scale structural changes in the dodecamer or within a monomer which are expected during an allosteric transition upon the binding of the inhibitor are not observed in these complexes. Of course, only small quaternary and tertiary changes were expected from crystal-soaking experiments because inhibitor soaks did not dissolve or crack GS crystals.

The movement of Asn-264 observed in the complexes GS–Glu, GS–Gln, GS–methionine sulfoximine, GS–Ser, GS–Ala, and GS–Gly could also support the common site for these effectors because, in our model, the amide group of Asn-264 collides with the α-amino group of these effectors. Moreover, engineered replacement of Arg-321 may provide further evidence for the common site, since the formation of hydrogen bonds between Arg-321 and these effectors may be important for their binding to GS. The replacement of Arg-321 by other amino acids (except possibly lysine) should result in lower binding of the substrate and of these inhibitors to GS.

Conclusion. Based on the crystal structures of GS–Ser, GS–Ala, GS–Gly, GS–Glu, and GS–(Glu+Ala) reported here, L-serine, L-alanine, and glycine bind to the L-glutamate site on unadenylylated GS–Mn from *S. typhimurium*, where they inhibit by competing for the substrate site. GS is regulated by multiple feedback inhibition but perhaps by a somewhat simpler mechanism than that proposed by Woolfolk and Stadtman (5).

We thank Drs. David Sigman, Paul Boyer, and Daniel Atkinson for helpful discussion on the interpretation of kinetic measurements; Dr. P. Boon Chock for comments on the manuscript; Dr. Daniel Anderson for helping with photography, the National Institutes of Health for support, and the San Diego Supercomputer Center for computing time.

1. Meister, A. (1980) in *Glutamine: Metabolism, Enzymology, and Regulation of Glutamine Metabolism*, eds. Palacios, R. & Mora, J. (Academic, New York), pp. 1–40.
2. Stadtman, E. R. & Ginsburg, A. (1974) in *The Enzymes*, ed. Boyer, P. (Academic, New York), Vol. 10, pp. 755–807.
3. Woolfolk, C. A. & Stadtman, E. R. (1964) *Biochem. Biophys. Res. Commun.* **17**, 313–319.
4. Woolfolk, C. A., Shapiro, B. M. & Stadtman, E. R. (1966) *Arch. Biochem. Biophys.* **116**, 177–192.
5. Woolfolk, C. A. & Stadtman, E. R. (1967) *Arch. Biochem. Biophys.* **118**, 736–755.
6. Ginsburg, A. (1969) *Biochemistry* **8**, 1726–1740.
7. Ross, P. D. & Ginsburg, A. (1969) *Biochemistry* **8**, 4690–4695.
8. Shrake, A., Parak, R. & Ginsburg, A. (1978) *Biochemistry* **17**, 658–664.
9. Rhee, S. G., Villafranca, J. J., Chock, P. B. & Stadtman, E. R. (1977) *Biochem. Biophys. Res. Commun.* **78**, 244–250.
10. Dahlquist, F. W. & Purich, D. L. (1975) *Biochemistry* **14**, 1980–1989.
11. Rhee, S. G., Chock, P. B. & Stadtman, E. R. (1978) *Front. Biol. Energ. Pap. Int. Symp.* **1**, 725–733.
12. Almassy, R. J., Janson, C. A., Hamlin, R., Xuong, N.-H. & Eisenberg, D. (1986) *Nature (London)* **323**, 304–309.
13. Yamashita, M. M., Almassy, R. J., Janson, C. A., Cascio, D. & Eisenberg, D. (1989) *J. Biol. Chem.* **264**, 17681–17690.
14. Janson, C. A., Almassy, R. J., Westbrook, E. M. & Eisenberg, D. (1984) *Arch. Biochem. Biophys.* **228**, 512–518.
15. Liaw, S., Jun, G. & Eisenberg, D. (1992) *Protein Sci.* **1**, 956–957.
16. Boyer, P. D., Mills, R. C. & Fromm, H. J. (1959) *Arch. Biochem. Biophys.* **81**, 249–263.
17. Levintow, L. & Meister, A. (1954) *J. Biol. Chem.* **209**, 265–280.
18. Ginsburg, A. (1972) *Adv. Protein Chem.* **26**, 1–79.
19. Meek, T. D. & Villafranca, J. J. (1980) *Biochemistry* **19**, 5513–5519.
20. Timmons, R. B., Rhee, S. G., Luterman, D. L. & Chock, P. B. (1974) *Biochemistry* **13**, 4479–4485.
21. Rhee, S. G. & Chock, P. B. (1975) *Biochemistry* **15**, 1755–1760.
22. Ginsburg, A., Gorman, E. G., Neece, S. H. & Blackburn, M. B. (1987) *Biochemistry* **26**, 5989–5996.
23. Sigman, D. S. & Glazer, A. N. (1972) *J. Biol. Chem.* **247**, 334–341.